FLIGHT PERFORMANCE OF MULTI-ROTOR CONFIGURATION TAIL ROTORS

Dong Han, donghan@nuaa.edu.cn, College of Aerospace Engineering, Nanjing University of Aeronautics and Astronautics, Nanjing 210016, China

Haoyun Wan, haoyunwan@nuaa.edu.cn, College of Aerospace Engineering, Nanjing University of Aeronautics and Astronautics, Nanjing 210016, China

George N. Barakos, George.Barakos@glasgow.ac.uk, CFD Laboratory, School of Engineering, University of Glasgow, G12 8QQ, Scotland, UK

Abstract

To better understand and predict the flight performance of multi-rotor configurations of tail rotors controlled via collective pitch or rotor speed, a flight performance tool is derived. The tool includes a tail rotor model, an aerodynamic interference model, and a trim method. The vertical configuration of a multi-rotor tail rotor can effectively take advantage of aerodynamic interference to reduce the required power. The five-rotor configuration with fixed rotor speed reduces the power by 36.7%. More rotors are preferable from the point of view of power consumption. Too many rotors are unnecessary, since the extra benefit obtained is very diminished. Varying the rotor speed is better for performance improvement compared with varying the collective pitch, since lower rotor speed leads to rotor power reduction. The five-rotor configuration with fixed collective pitch reduces the power by 53.3%. The severe aerodynamic interference between the rotors leads to the longitudinal configuration of multi-rotor configuration having much poorer performance. The four-rotor configuration in a “plus” arrangement achieves better performance than the cross four-rotor configuration or a vertical four-rotor configuration.

NOMENCLATURE

c	blade chord length, m
C_l	lift coefficient, dimensionless
C_d	drag coefficient, dimensionless
D	drag, N
k	cross-induced velocity factor, dimensionless
L	lift, N
N_b	number of blades
N_R	number of rotors
r	radial coordinate, m
P	rotor power, W
Q	rotor torque, Nm
R	tail rotor radius, m
T	thrust, N
U	resultant velocity, m/s
v_i	induced velocity, m/s
w	damper factor, dimensionless
γ_j	wake skew angle, rad
η	power reduction, dimensionless
θ_0	collective pitch, rad
κ_i	self-induced velocity factor, dimensionless
ρ	air density, kg/m^3
ψ	azimuth angle, rad
Ω	tail rotor speed, rad/s

Subscript

i	rotor index
n	iteration number
NR	related with N_R rotor configuration

Superscript

$\bar{()}$	$()/R$

1. INTRODUCTION

Future environmental and operational requirements will become stricter for helicopters. One way to improve the situation is by introducing more electric vehicles [1]. Electric driven tail rotors, as an example, have the benefits of performance improvement, weight decrease, noise reduction, easier and reduced maintenance, and so on [2], and some helicopter designs begin to use them [2-4]. However, electrification of helicopter tail rotors leads to a wider design space. More rotors, not just one rotor, can be used to balance the main rotor torque. For example, the modified Bell Model 429 helicopter uses an Electrically Distributed Anti-Torque System (EDAT), which has four smaller rotors.

Electric driven rotors are usually different from conventional helicopter main or tail rotors. Electric motors offer rotor speed control instead of blade pitch, which can simplify the rotor system. From the

point of view of performance, varying the rotor speed is an effective way to reduce the rotor power consumption [5-9]. The removal of the pitch control system may also reduce the weight of the rotor system and increase its reliability.

Multiple rotors can be used to form different multi-rotor configurations. For example, quadrotor aircraft can have a cross (x) or a plus (+) configuration. Using more rotors leads to even more configurations. The wakes trailed from the rotors interfere with each other, which affects their aerodynamic performance. This interference may benefit the rotors or degrade their aerodynamic performance [10-13]. Consequently, choosing the right configuration becomes an important topic for multi-rotor systems.

This work concentrates on the flight performance of multi-rotor tail configurations. Several configurations are analyzed, and their power consumptions are compared. The effect of the control means of changing the collective pitch or rotor speed on the performance of multi-rotor configuration tail rotors is investigated.

2. FLIGHT PERFORMANCE MODEL

2.1. Modeling Approach

The blades of tail rotors are assumed to be rigid with no blade flapping allowed. The blade element method is used to predict the performance of the rotors. The tail rotor thrust and power are obtained by numerically integrating the forces acting on the blade elements along the blade radius and azimuth with uniform inflow, as shown in Fig. 1. The tail rotor thrust is

$$T = \frac{N_b}{2\pi}\int_0^{2\pi}\int_0^R \left(dL\cos\phi - dD\sin\phi\right)drd\psi = \frac{N_b}{2\pi}\int_0^{2\pi}\int_0^R \frac{1}{2}\rho U^2 c\left(C_l\cos\phi - C_d\sin\phi\right)drd\psi \quad (1)$$

where, N_b is the number of blades, R the tail rotor radius, L the lift, D the drag, ρ the air density, U the resultant velocity at a blade element, c the blade chord length, C_l the lift coefficient, C_d the drag coefficient, r the radial coordinate, and ψ the azimuth angle. Look-up airfoil aerodynamic tables are used to calculate the lift C_l and drag coefficients C_d of the blade elements according to the local resultant air flow and angle of attack. The tail rotor torque is calculated by

$$Q = \frac{N_b}{2\pi}\int_0^{2\pi}\int_0^R r\left(dL\sin\phi + dD\cos\phi\right)drd\psi = \frac{N_b}{2\pi}\int_0^{2\pi}\int_0^R \frac{1}{2}\rho U^2 c\left(C_l\sin\phi + C_d\cos\phi\right)rdrd\psi \quad (2)$$

and the corresponding tail rotor power is

$$P = Q\Omega \quad (3)$$

where, Ω is the tail rotor speed. Validation of the employed tail rotor model can be found in Ref. 9.

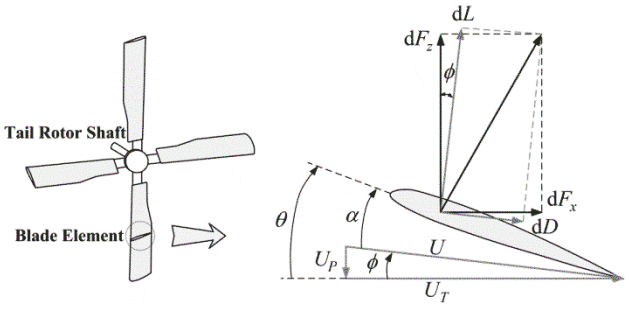

Figure 1 Aerodynamic environment at the tail rotor blade element.

2.2. Aerodynamic Interference Model

A theoretical formula on the basis of the Biot-Savart law is used to predict the aerodynamic interference between the rotors [14]. This method has been extended to consider the aerodynamic interference between multiple rotors in forward flight. A horseshoe vortex is trailed from each of the retreating and advancing sides, as shown in Fig. 2. This aerodynamic interference model assumes that the horseshoe vortex trailed from one rotor generates an additional induced velocity to other rotors. If a point lies between the two vortices and downstream the incoming flow, both vortices induce downwash velocities. If a rotor lies at this location, its performance may be degraded. If the point is located outside the vortices and downstream the incoming flow, the closer vertex induces a larger upwash velocity than other vortices located further away. The resultant velocity at this point is upwash, which reduces the angle of attack of the rotor, and improves the rotor performance.

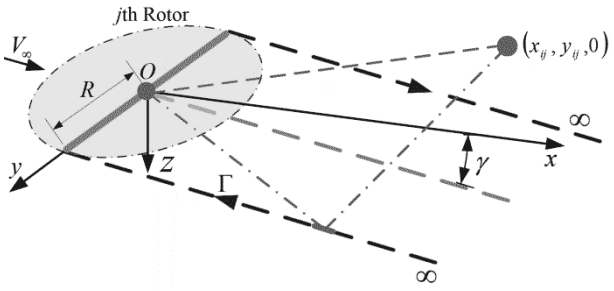

Figure 2 Coordinate system.

It is assumed that the velocity induced by a rotor on another is uniform, and the rotors are on the same plane. The induced velocity at the rotor

hub center can denote the aerodynamic interaction. For a multi-rotor system, the induced velocity over the rotors can be expressed as

$$(4)\qquad \begin{Bmatrix} v_i^{(1)} \\ v_i^{(2)} \\ v_i^{(3)} \\ \vdots \\ v_i^{(n)} \end{Bmatrix} = \begin{bmatrix} \kappa_1 & k_{12} & k_{13} & \cdots & k_{1n} \\ k_{21} & \kappa_2 & k_{23} & \cdots & k_{2n} \\ k_{31} & k_{32} & \kappa_3 & \cdots & k_{3n} \\ \vdots & \vdots & \vdots & \ddots & \vdots \\ k_{n1} & k_{n2} & k_{n3} & \cdots & \kappa_n \end{bmatrix} \begin{Bmatrix} v_{i0}^{(1)} \\ v_{i0}^{(2)} \\ v_{i0}^{(3)} \\ \vdots \\ v_{i0}^{(n)} \end{Bmatrix}$$

where the subscript '0' denotes the velocity of an isolated rotor. κ_i is the correction factor for self-induced losses of a real rotor. k_{ij} denotes the cross-induced velocity factor generated by the *j*th rotor to the *i*th rotor, and it can be expressed as

$$(5)\qquad k_{ij} = \frac{1}{2}\left[\frac{\left(\bar{y}_{ij}+1\right)\left(1+\dfrac{\bar{x}_{ij}\cos\gamma_j}{\sqrt{\bar{x}_{ij}^2+\left(\bar{y}_{ij}+1\right)^2}}\right)}{\left(\bar{y}_{ij}+1\right)^2+\bar{x}_{ij}^2\sin^2\gamma_j} - \frac{\left(\bar{y}_{ij}-1\right)\left(1+\dfrac{\bar{x}_{ij}\cos\gamma_j}{\sqrt{\bar{x}_{ij}^2+\left(\bar{y}_{ij}-1\right)^2}}\right)}{\left(\bar{y}_{ij}-1\right)^2+\bar{x}_{ij}^2\sin^2\gamma_j} \right]$$

where, $\bar{x}_{ij}$ and $\bar{y}_{ij}$ are the dimensionless coordinates of the hub center of the *i*th rotor relative to the hub center of the *j*th rotor, as shown in Fig. 2. γ_j is the wake skew angle between the *j*th rotor disk and the corresponding trailed vortex plane. The non-dimensional expressions are defined as

$$(6)\qquad \begin{cases} \bar{x}_{ij} = \dfrac{x_{ij}}{R} \\ \bar{y}_{ij} = \dfrac{y_{ij}}{R} \end{cases}$$

2.3. Trimming Approach

Tail rotors generate specific thrust to balance the main rotor torque. For the convenience of performance comparison of multi-rotor configuration tail rotors, the multiple rotors are trimmed to generate a prescribed resultant thrust. It is assumed that all the smaller rotors have the same collective pitch and rotor speed.

For a prescribed thrust T_p, if the tail rotor uses the collective pitch to control the thrust, the iterative equation to obtain the converged solution is

$$(7)\qquad \left(\theta_0\right)_{n+1} = \left(\theta_0\right)_n + w\left[T_p - \left(T\right)_n\right] / \left(\frac{\partial T}{\partial \theta_0}\right)_n$$

where, θ_0 is the collective pitch, and the subscript *n* denotes the value at the nth step. *w* is a numerical damping factor to enhance the convergence of the iteration and reduce the computation time (a value of 0.5 is used here). The total rotor thrust *T* is obtained by

$$(8)\qquad T = \sum_{i=1}^{N_R} T_i$$

where, the subscript *i* denotes the index of a smaller rotor of the multi-rotor configuration. Similarly, if the tail rotor uses the rotor speed to control the thrust, the iterative equation to obtain the converged solution is

$$(9)\qquad \left(\Omega\right)_{n+1} = \left(\Omega\right)_n + w\left[T_p - \left(T\right)_n\right] / \left(\frac{\partial T}{\partial \Omega}\right)_n$$

3. VERTICAL CONFIGURATION

3.1. Parameters of the Employed Configuration

For convenience of performance comparison, the multi-rotor configurations have the same blade tip speed as the conventional single-rotor configuration. The sum of the rotor disk areas of the multi-rotor configuration equals the single-rotor value, and the sum of the blade planform areas also equals the single-rotor configuration. The other parameters remain unchanged. The following equations can be used to calculate the rotor radius R_{NR}, rotor speed Ω_{NR} and blade chord c_{NR} of the corresponding multi-rotor configuration tail rotor with N_R smaller rotors:

(10)
$$\begin{cases} R_{NR} = R/\sqrt{N_R} \\ \Omega_{NR} = \Omega/\sqrt{N_R} \\ c_{NR} = c/\sqrt{N_R} \end{cases}$$

where, R is the rotor radius of the single-rotor configuration, Ω the rotor speed, and c the blade chord. The power reduction is defined as

(11)
$$\eta = \left(1 - \frac{P_n}{P_1}\right) \times 100\%$$

where, P_n denotes the total power with n rotors, and P_1 is the power of the single-rotor configuration. This is used to show the advantage or disadvantages of multi-rotor tail configurations in power saving.

The tail rotor of the UH-60A helicopter is used as the baseline single-rotor configuration. Its parameters are listed in Table 1. In the following analysis, the forward speed is 100km/h and the corresponding total rotor thrust is 4900N.

Table 1 The tail rotor parameters of UH-60A helicopter [16].

Tail Rotor Radius	1.68 m
Nominal Tail Rotor Speed	124.6 rad/s
Tail Rotor Blade Chord	0.25 m
Tail Rotor Blade Twist	-18^o
Airfoil	SC1095
Number of Blades	4

3.2. Fixed Rotor Speed

The vertical multi-rotor configuration is investigated, and its smaller rotors are vertically distributed, as shown in Fig. 3. The parameters of this configuration with different numbers of rotors are shown in Fig. 4. The distance between two adjacent rotors is assumed to be two times their rotor radius. In this case, all the rotors have the same rotor speed, and use the same collective pitch to control their thrusts. In this configuration, each smaller rotor is outside the wakes trailed from the other rotors. So, aerodynamic interference will induce upwash to this rotor, which can improve its aerodynamic performance and reduce its power consumption.

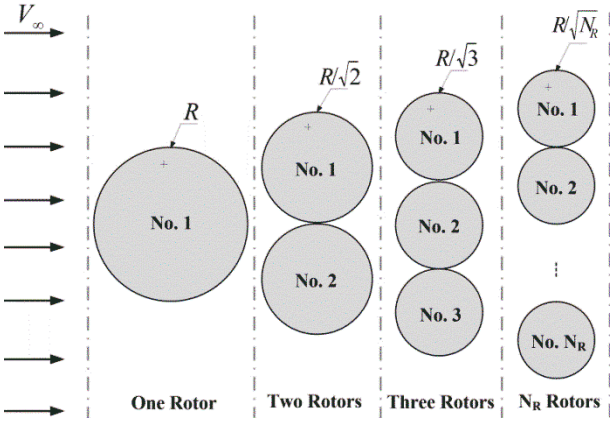

Figure 3 Vertical configuration of multi-rotor configuration tail rotor.

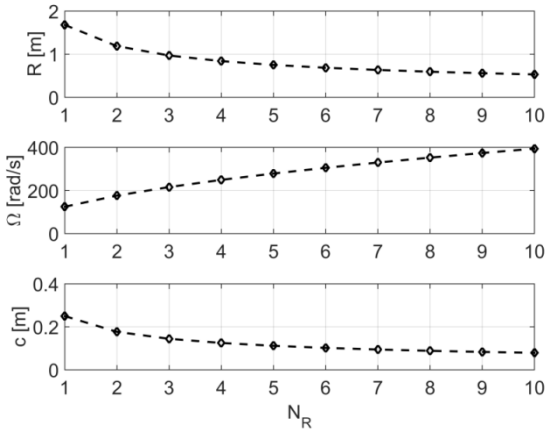

Figure 4 Rotor parameters for the different rotor configurations.

For the configurations with different number of rotors, the power consumptions are shown in Fig. 5. It is obvious that, without considering aerodynamic interferences, the configurations have almost the same power consumption. With the aerodynamic interference, the total power can be reduced. The two-rotor configuration reduces the total power consumption by 19.2%, and the five-rotor configuration by 36.7%. With the increase in the number of rotors, the benefit increases, and the increment of the power reduction decreases. It is not necessary to use too many rotors due to the much lower power saving increment. With the increase in the number of rotors, the size of the tail also increases, which may lead to problems such as structural weight, strength, reliability, maintainability and so on.

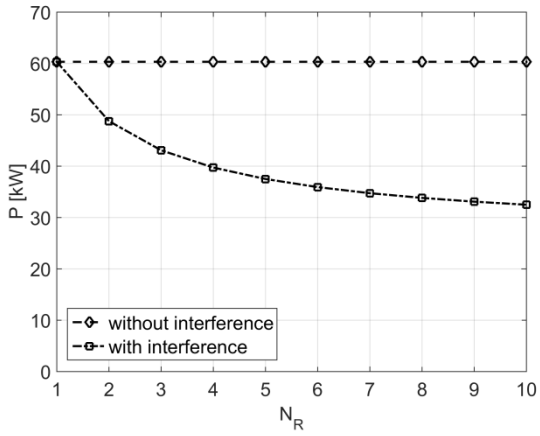

Figure 5 Total power required for the different rotor configurations.

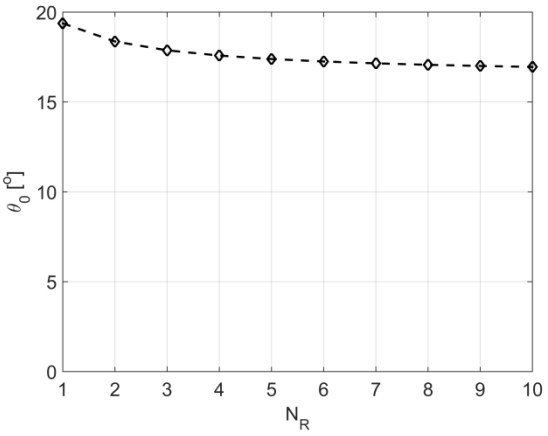

Figure 6 Collective pitch angles.

Figure 6 shows the collective pitches for the configurations with different number of rotors. Increasing the number of rotors decreases the collective pitch, which is beneficial to the design of rotor control system. Since each rotor generates upwash to the other rotors due to the aerodynamic interference, the collective pitch can be reduced to generate the same thrust. This confirms the positive effect of the aerodynamic interference between the rotors on the performance improvement of this configuration tail rotor.

Table 2 lists the distribution of the rotor thrusts of the configurations with different number of rotors. Since the vertical configuration is symmetric about the middle rotor, the thrust distribution is also symmetric. The middle rotor generates the largest thrust, and the outmost two rotors provide the lowest thrust. The relative difference between the maximum and minimum values increases with the number of rotors. For the three-rotor configuration, the maximum thrust is 1.12 times the minimum value. For the ten-rotor configuration, the ratio changes to 1.29. Excessive thrust difference between the rotors will affect the overall performance of the tail rotor, and the potential of some smaller rotors is difficult to be utilized.

Table 2 Distribution of rotor thrust.

N_R	i									
	1	2	3	4	5	6	7	8	9	10
1	4899.9									
2	2450.0	2450.0								
3	1570.7	1758.7	1570.7							
4	1137.6	1312.5	1312.5	1137.6						
5	884.8	1032.9	1064.7	1032.9	884.8					
6	720.8	846.3	882.9	882.9	846.3	720.8				
7	606.5	714.3	749.7	758.8	749.7	714.3	606.5			
8	522.7	616.7	649.4	661.2	661.2	649.4	616.7	522.7		
9	458.7	541.9	571.7	584.0	587.4	584.0	571.7	541.9	458.7	
10	408.4	482.8	510.0	522.0	526.8	526.8	522.0	510.0	482.8	408.4

3.3. Fixed Collective Pitch

Electric driven rotors usually use variable rotor speed to control their thrusts. A prescribed collective pitch of 19.38^{o} is used, which equals to the value of the single-rotor configuration at fixed rotor speed.

The total power and corresponding power reduction are shown in Fig. 7. The total power decreases with the number of rotors. The corresponding power reduction increases with the number of rotors, and the increment of the power reduction decreases. For the two-rotor configuration, the total power is reduced by 28.7%, and for the five-rotor configuration by 53.3%. For the ten-rotor configuration, the total power with fixed collective pitch is 68.6% of the power with fixed

rotor speed. It is obvious that using variable rotor speed can obtain more power savings.

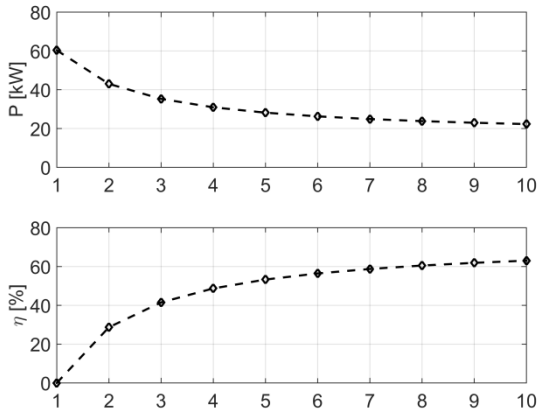

Figure 7 Rotor power and corresponding power reduction.

Figure 8 shows the rotor speeds for the tail rotors using different control methods. Due to the positive effect of aerodynamic interference, the rotor speed decreases when compared with the configurations with fixed rotor speeds. For the ten-rotor configuration, the rotor speed decreased by 23.7%. This large reduction of rotor speed significantly decreases the tail rotor power. The mechanism of the reduction is discussed in Ref. 9. It can be concluded that the aerodynamic interference and variable rotor speed dominate the power saving and performance improvement of the vertical multi-rotor configuration tail. However, it is necessary to point out that a wide range change of rotor speed will inevitably bring structural and dynamic problems.

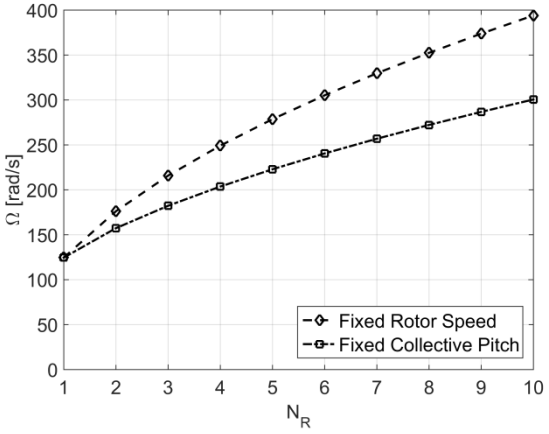

Figure 8 Comparison of rotor speed.

Table 3 lists the distribution of the rotor thrusts of the configurations with fixed collective pitch. The trend shown in Table 3 is similar to that of Table 2. The outer rotors generate lower thrust than the inner rotors. For the ten-rotor configuration, the maximum thrust is 1.22 times the minimum value. The distribution of thrust is more uniform than that of the configuration with fixed rotor speed.

Table 3 Distribution of rotor thrust with fixed collective pitch.

N_R	*i*									
	1	2	3	4	5	6	7	8	9	10
1	4900.0									
2	2450.0	2450.0								
3	1576.1	1747.8	1576.1							
4	1147.6	1302.4	1302.4	1147.6						
5	897.8	1026.3	1051.8	1026.3	897.8					
6	735.6	843.0	871.4	871.4	843.0	735.6				
7	622.2	713.7	740.6	747.2	740.6	713.7	622.2			
8	538.6	618.0	642.5	650.9	650.9	642.5	618.0	538.6		
9	474.6	544.5	566.7	575.3	577.7	575.3	566.7	544.5	474.6	
10	424.1	486.4	506.5	514.9	518.1	518.1	514.9	506.5	486.4	424.1

Figure 9 shows the total power and the corresponding rotor speed for different prescribed rotor collective pitch angles. The rotor power decreases significantly with the increase in the prescribed collective pitch first, and then increases. An optimum prescribed collective exists at this flight state, which indicates that too high or too low collective pitch is not preferred. The rotor speed decreases with the increase in the collective pitch, and too low rotor speed is not preferred. The rotor speed reduces by more than 50%, if the collective is increased from 16^o to 24^o.

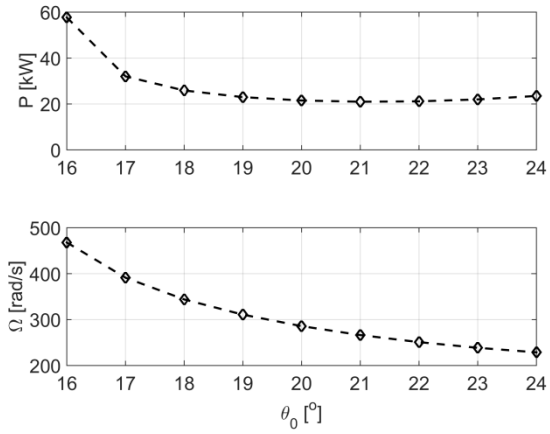

Figure 9 Total power with different collective pitches.

4. LONGITUDINAL CONFIGURATION

The vertical multi-rotor configuration tail can take full advantage of the aerodynamic interference between the smaller rotors, since one rotor is outside of the wakes trailed from the other rotors. If the multi-rotor configuration tail rotor uses a longitudinal distribution of rotors shown in Fig. 10, the aerodynamic interference can have negative effect on the aerodynamic performance of the rotors. The distance between adjacent two rotors is also assumed to be two times the rotor radius. Due to the side effect of aerodynamic interference, the rotors have to use larger collective pitch to maintain enough thrust. The prescribed collective pitch of the rotors is set to 25°.

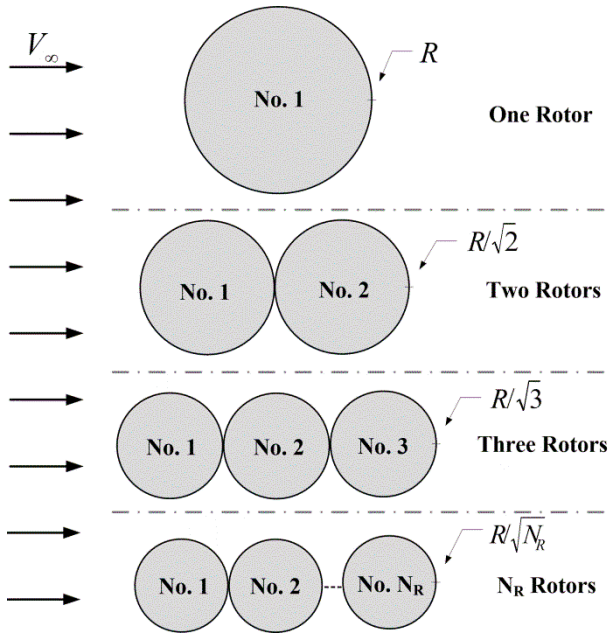

Figure 10 Longitudinal configuration of multi-rotor configuration tail rotor.

Figure 11 shows the rotor power and corresponding power reduction for the configurations with different number of rotors. With the increase in the number of rotors, the total power consumption increases. The total power of the ten-rotor configuration is 3.84 times that of the one-rotor configuration. In general, rotors should not be placed between the wakes trailed from the other rotors. Otherwise, severe downwash can be induced, which can significantly degrade the aerodynamic performance. The side effect of the aerodynamic interference of the longitudinal configuration is very obvious. This type of multi-rotor configuration is not suitable for tail rotors

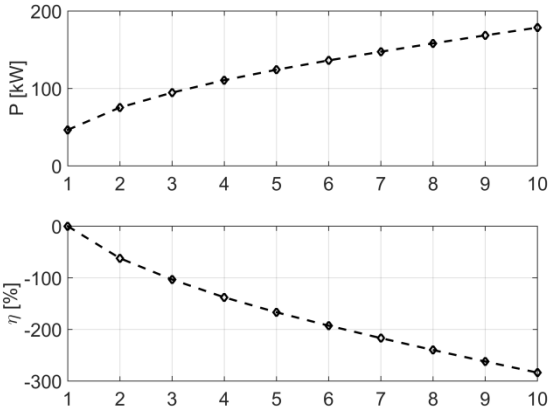

Figure 11 Rotor power and corresponding power reduction.

Table 4 lists the distribution of rotor thrusts for the longitudinal configuration. The trend shown in Table 4 is different from that in Table 2 or 3. The foremost rotor generates the largest thrust, and the last rotor provides the lowest thrust. For the ten-rotor configuration, the thrust generated by the foremost rotor is 4.37 times that of the last rotor. It is obvious the strongest aerodynamic interference appears at the last rotor.

Table 4 Distribution of rotor thrust for the longitudinal configuration.

N_R	i									
	1	2	3	4	5	6	7	8	9	10
1	4900.0									
2	3301.1	1598.9								
3	2583.6	1268.5	1047.9							
4	2184.0	1106.8	880.1	729.1						
5	1911.8	994.3	782.4	637.2	574.3					
6	1711.6	909.1	712.3	584.0	510.7	472.2				
7	1555.5	841.0	657.9	543.5	474.4	425.2	402.5			
8	1429.1	784.4	613.7	510.3	446.0	399.2	365.6	351.8		
9	1323.9	736.2	576.6	482.1	422.3	378.5	345.8	321.4	313.2	
10	1234.8	694.4	544.8	457.5	401.7	360.9	329.9	305.7	287.4	282.8

5. FOUR-ROTOR CONFIGURATION

The previous analyses indicate that too many rotors are not necessary, a four- or a five-rotor configuration balances performance and number of rotors. Usually, four rotors can form a 'cross' or a 'plus' configuration, as shown in Fig. 12. In the following analysis, the distance between two adjacent rotors is also assumed to be two times the rotor radius. For these two configurations, the rotor speed is used to control the thrust. A prescribed collective pitch of 19.38^o is used in the following analysis.

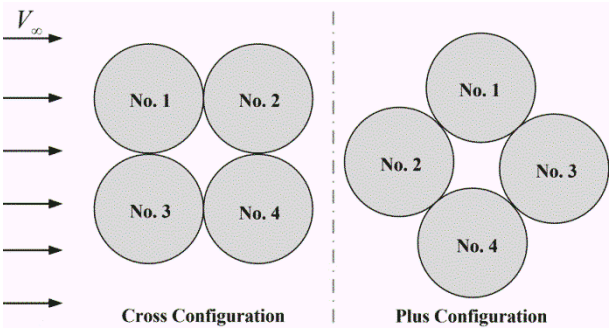

Figure 12 Four rotor configurations.

Figure 13 shows the individual rotor power for the cross and plus configurations. For the cross configuration, Rotors 1 and 3 have the same power consumption, and the same holds for Rotors 2 and 4. Rotor 2 has lower power consumption than that of Rotor 1. For the plus configuration, Rotor 2 has the higher power consumption, and Rotor 1 has the lower. Rotor 4 has the same power consumption as Rotor 1 due to the symmetry of the configuration. The total power consumption of the cross configuration is 74.0kW, which is 2.39 times the value of the vertical four-rotor configuration. However, the power consumption of the plus configuration is 83.8% of the vertical four-rotor configuration. It is obvious that the plus configuration achieves the best performance, since its can more effectively take advantage of aerodynamic interference.

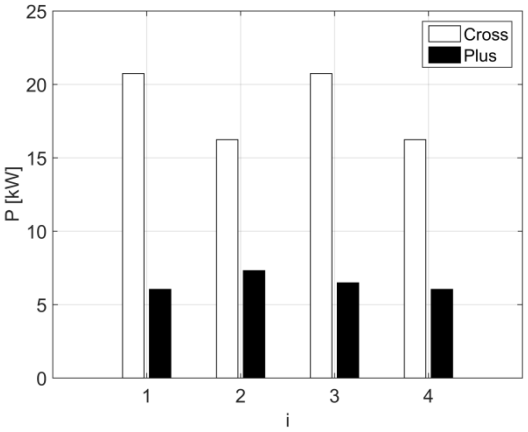

Figure 13 Individual rotor power for the assessed four-rotor configurations.

Figure 14 shows the individual rotor thrust of the two four-rotor configurations. For the cross configuration, Rotors 1 and 3 generate much larger thrust than Rotors 2 and 4. The front rotor has better aerodynamic performance than the rear rotor. For the plus configuration, Rotors 1 and 4 generate identical and larger thrust, and Rotor 2 generates the lowest thrust. The front rotor has poorer performance.

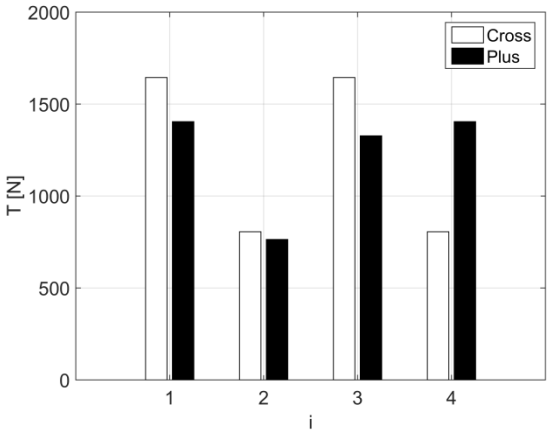

Figure 14 Individual rotor thrust of the two four-rotor configurations.

6. CONCLUSIONS

To analyze the flight performance of multi-rotor tail configurations, a performance model considering the aerodynamic interference between the rotors is derived. An iterative algorithm is proposed to obtain the converged solution of the control variable (collective pitch or rotor speed) for a given total thrust. The analyses yielded the following conclusions:

1) The vertical multi-rotor configuration can effectively take advantage of the aerodynamic interference to reduce the total power consumption and improve performance.

2) For the vertical multi-rotor configuration, a large number of rotors is preferred from the point of view of power consumption. Too many rotors are unnecessary, since the extra benefit obtained is diminishing with the increase in the number of rotors.

3) For the vertical multi-rotor configuration, varying the rotor speed is better for performance compared to varying the collective pitch.

4) The longitudinal multi-rotor configuration has poorer performance than the vertical configuration due to the side effects of aerodynamic interference between the rotors.

5) The plus (+) four-rotor configuration achieves better performance than the cross (x) four-rotor configuration.

6) Aerodynamic interference and variable rotor speed dominate the performance improvement of multi-rotor tail configurations.

ACKNOWLEDGMENTS

This work is supported from the National Natural Science Foundation of China (11972181), and the Six Talent Peaks Project in Jiangsu Province (GDZB-013).

REFERENCES

[1] Serafini, J., Cremaschini, M., Bernardini, G., Solero, L., Ficuciello, C., and Gennaretti, M., “Conceptual All-Electric Retrofit of Helicopters: Review, Technological Outlook, and a Sample Design,” IEEE Transactions on Transportation Electrification, Vol. 5, No. 3, 2019, pp. 782-794.

[2] Zhang, Y., Jiang, C., Wang, Y., Sun, F., Wang, H., “Design and Application of an Electric Tail Rotor Drive Control (ETRDC) for Helicopters with Performance Tests,” Chinese Journal of Aeronautics, Vol. 39, No. 1, 2018, pp. 1894-1901.

[3] Mellor, P. H., Yon, J., Williamson, S., Farman, J., Booker, J. D., Barber, M., Stickels, K., Brinson, P., “Electrical Machine Technologies for an Electric Tail rotor Drive,” 41st European Rotorcraft Forum, September 1-4, 2015, Munich, Germany.

[4] Stickels, K., Brunetti, M., Barber, M., Manimala, B., Brinson, P., Roe, T., Mellor, P. H., Booker, J. D., Williamson, S. J., and Yon, J., “Advances in Helicopter Electric Tail Rotor Drive,” 43rd European Rotorcraft Forum, Milan, Italy, September 12- 15, 2017.

[5] Kang, H., Saberi, H., Gandhi, F., “Dynamic Blade Shape for Improved Helicopter Rotor Performance,” Journal of the American Helicopter Society, Vol. 55, No. 3, 2010, pp. 0320081-03200811.

[6] Mistry, M., and Gandhi, F., “Helicopter Performance Improvement with Variable Rotor Radius and RPM,” Journal of the American Helicopter Society, Vol. 59, No. 4, 2014, pp. 042010.

[7] Misté, G. A., and Benini, E., “Variable-speed rotor helicopters: Performance Comparison between Continuously Variable and Fixed-ratio Transmissions,” Journal of Aircraft, Vol. 53, No. 5, 2016, pp. 1189-1200.

[8] Han, D., Pastrikakis, V. and Barakos, G. N., “Helicopter Performance Improvement by Variable Rotor Speed and Variable Blade Twist,” Aerospace Science and Technology, Vol. 54, 2016, pp.164-173.

[9] Han, D., and Barakos, G. N., “Variable-speed Tail Rotors for Helicopters with Variable-speed Main Rotors,” Aeronautical Journal, Vol. 121, No. 1238, 2017, pp. 433-448.

[10] Hwang, J. Y., Jung, M. K., and Kwon, O. J., Numerical Study of Aerodynamic Performance of a Multirotor Unmanned-Aerial-Vehicle Configuration, Journal of Aircraft, Vol. 52, No. 3, 2015, pp. 839-846.

[11] Nguyen, D. H., Liu, Y., and Mori, K., “Experimental Study for Aerodynamic

Performance of Quadrotor Helicopter," Transactions of the Japan Society for Aeronautical and Space Sciences, Vol. 61, No. 1, 2018, pp. 29-39.
[12] Misiorowski, M. and Gandhi, F. "Computational Study on Rotor Interactional Effects for a Quadcopter in Edgewise Flight," AIAA Journal, Vol. 57, No. 12, 2019, pp. 5309-5319.
[13] Han, D., Zhou, L., and Barakos, G. N., "Parametric Investigation of the Flight Performance of a Variable Pitch X-Configuration Quadrotor Aircraft, Journal of Aerospace Engineering, Doi: 10.1061/(ASCE)AS.1943-5525.0001481.
[14] Han, D., and Barakos, G. N., "Aerodynamic Interference Model for Multirotors in Forward Flight," Journal of Aircraft, Vol. 57, No. 6, 2020, pp. 1220-1223.
[15] Hilbert, K. B., "A Mathematical Model of the UH-60 Helicopter," Technical Report NASA-TM-85890, 1984.